

Evaluation of Lipid Exposure of Tryptophan Residues in Membrane Peptides and Proteins

Alexey S. Ladokhin¹

Departments of Physiology and Biophysics and Program in Macromolecular Structure, University of California, Irvine, California, 92697-4560

Received June 7, 1999

Fluorescence quenching is used to gain information on the exposure of tryptophan residues to lipid in membrane-bound proteins and peptides. A protocol is developed to calculate this exposure, based on a comparison of quenching efficiency and of a fluorescence lifetime (or quantum yield) measured for a protein and for a model tryptophan-containing compound. Various methods of analysis of depth-dependent quenching are compared and three universal measures of quenching profile are derived. One of the measures, related to the area under profile, is used to estimate quenching efficiency. The method is applied to single tryptophan mutants of a membrane-anchoring nonpolar peptide of cytochrome *b₅* and of an outer membrane protein A. Analysis of quenching of the cytochrome's nonpolar peptide by a set of four brominated lipids reveals a temperature-controlled reversible conformational change, resulting in increased exposure of tryptophan to lipid and delocalization of its transverse position. Kinetic quenching profiles and fluorescence binding kinetics reported by Kleinschmidt *et al.* (*Biochemistry* (1999) 38, 5006–5016) were analyzed to extract information on the relative exposure of tryptophan residues during folding of an outer membrane protein A. Trp-102, which translocates across the bilayer, was found to be noticeably shielded from the lipid environment throughout the folding event compared to Trp-7, which remains on the *cis* side. The approach described here provides a new tool for studies of low-resolution structure and conformational transitions in membrane proteins and peptides.

© 1999 Academic Press

Determination of membrane organization and dynamics is one of the most challenging problems of structural biology because many methods (even of low resolution) developed for water-soluble systems are not directly applicable to membranes. For example, while the position of fluorescence spectrum of tryptophan in a globular protein indicates a degree of exposure to the aqueous phase, it will not be sensitive to exposure to the lipid phase in a membrane-bound protein. Therefore, new approaches should be developed for structural studies in membranes. Here a method of evaluation of tryptophan exposure to lipids based on fluorescence quenching is presented.

The depth-dependent fluorescence quenching technique is a useful tool to explore the structure of membrane proteins and peptides along the depth coordinate (1–7). To achieve this objective it utilizes lipids with bromine atoms or spin labels selectively attached to certain positions along acyl chains. The parallax method, PM² (8, 9), and distribution analysis, DA (10–12), can be utilized to quantitate the quenching to extract information on membrane penetration. This study focuses on the determination of the exposure of the tryptophan sidechain in membrane proteins and peptides to the lipid phase.

First, the connection between the parameters of DA and PM and universal measures of experimentally observed quenching profile is established. It is demon-

² Abbreviations used: POPC, palmitoylphosphatidylcholine; 4-5, 6-7, 9-10, or 11-12BPC, 1-palmitoyl-2-(dibromostearoyl)-phosphatidylcholine with bromine atoms at the 4-5, 6-7, 9-10, or 11-12 positions, respectively; quenching profile or profile, depth-dependent fluorescence quenching profile; TOE, tryptophan octyl ester; NPP, nonpolar peptide of the cytochrome *b₅* (-103, -108, -112) mutant of Tretyachenko-Ladokhina, V. G., Ladokhin, A. S., Wang, L., Steggles, A. W., and Holloway, P. W. (1993) *Biochim. Biophys. Acta* 1153, 163–169; OmpA, outer membrane protein A; DA, distribution analysis; PM-2, two-parameter parallax method; PM-3, three-parameter parallax method.

¹ On leave from the Institute of Molecular Biology and Genetics, National Academy of Sciences of Ukraine, Kiev 252143, Ukraine.

TABLE 1

Results of the Application of Different Types of Analysis to Tryptophan Fluorescence Quenching in Membranes

Probe or peptide	DA			PM-2		PM-3		<i>f</i>
	h_m (Å)	σ (Å)	<i>S</i>	h_m (Å)	R_c (Å)	h_m (Å)	R_c (Å)	
TOE, +20°C	11.3	5.5	18.9	10.3	5.8	11.4	8.9	0.38
TOE, +40°C	11.1	5.5	21.8	10.4	6.1	11.3	8.9	0.44
TOE, +60°C	11.0	5.7	24.6	10.3	6.4	11.0	9.0	0.47
<i>b</i> ₅ rabbit	11.1	4.8	14.2	10.3	5.4	11.0	7.3	0.51
<i>b</i> ₅ (-108, -112)	10.1	4.4	15.3	9.9	5.7	10.0	6.7	0.67
<i>b</i> ₅ (-103, -108, -112)	9.5	3.4	13.9	9.5	5.9	9.5	5.4	1.24
NPP, +20°C	9.5	5.0	21.6	9.5	6.3	9.5	7.6	0.67
NPP, +60°C	10.7	7.1	32.5	9.9	6.7	10.3	11.3	0.32
NPP, +20°C back	9.6	5.1	23.4	9.6	6.5	9.5	7.7	0.68
Melittin, +20°C	10.0	3.7	17.1	10.0	6.3	10.0	5.7	1.27
Melittin, +45°C	10.3	4.2	19.2	10.2	6.4	10.2	6.4	0.98
Melittin, +20°C back	9.7	3.2	15.7	9.7	6.3	9.7	5.1	1.71

Note. Original data for TOE, *b*₅, and melittin were published previously (13, 14, 17). NPP data were obtained as described under Materials and Methods.

strated that either method, when used with three fitting parameters, produces similar results. The method is then applied to fluorescence quenching of a membrane-anchoring nonpolar peptide (NPP) of cytochrome *b*₅ mutant (-103, -108, -112) (13) and two single tryptophan mutants (Trp-7 and Trp-102) of an outer membrane protein A (OmpA) (7). Temperature-controlled and kinetic changes in exposure of tryptophan residues are quantitated in case of NPP and OmpA, respectively.

MATERIALS AND METHODS

POPC was obtained from Avanti Polar-Lipids, Inc. (Pelham, AL) and BRPCs were synthesized as described by Markello *et al.* (1). Lipid vesicles were prepared by sonication. DL-Tryptophan octyl ester (TOE) was from Sigma Chemical Co. (St. Louis, MO). Hepes buffer (10 mM) containing 0.1 mM EDTA, pH 7.1, was used. The sample contained 2 mM POPC and 10 μM of NPP or 5 μM of TOE. Steady-state fluorescence measurements were made with an SLM 8000c spectrofluorometer (Urbana, IL). An excitation of 280 nm was used; both excitation and emission slits were 4 nm. Normally from 5 to 15 spectra were averaged to get an adequate signal-to-noise ratio. The rest of the experimental conditions were as described previously (14). Fluorescence quantum yield was determined relative to membrane bound TOE at 20°C. Data were collected at 20°C, and then samples were heated to 60°C and new data sets were collected. After that samples were brought back to 20°C and new data sets were collected,

designated in Table 1 as “20°C back.” Samples were incubated at each temperature for an hour before any data were collected.

THEORY

In a depth-dependent fluorescence quenching experiment one determines the fluorescence intensity, *F*, of a probe as a function of the known depth of the quencher, *h*. Data are usually normalized to the intensity in the absence of quenching, *F*₀. Below various methods of quantitating membrane quenching, such as Distribution Analysis (DA), and two- and three-parameter Parallax Method (PM-2 and PM-3, respectively) (8, 11) are compared. The principal equations for these methods, rewritten in a similar form for ease of comparison, are

DA:

$$\ln \frac{F_0}{F(h)} = \frac{S}{\sigma \sqrt{2\pi}} \cdot \exp \left[-\frac{(h - h_m)^2}{2\sigma^2} \right] \quad [1]$$

PM-2:

$$\ln \frac{F_0}{F(h)} = \pi \cdot C \cdot [R_c^2 - (h - h_m)^2], \quad h - h_m < R_c$$

$$\ln \frac{F_0}{F(h)} = 0, \quad h - h_m \geq R_c \quad [2]$$

PM-3:

$$\ln \frac{F_0}{F(h)} = \pi \cdot C \cdot f \cdot [R_c^2 - (h - h_m)^2], \quad h - h_m < R_c$$

$$\ln \frac{F_0}{F(h)} = 0, \quad h - h_m \geq R_c \quad [3]$$

For simplicity of presentation only, the case when concentrations of different quenchers are equal to each other is considered (general case will require correction factors described previously (11)). The expression on the left-hand side will be called the depth-dependent fluorescence quenching profile.

On the right are analytical expressions for the quenching profile represented by either a Gaussian function (DA) or truncated parabola (PM-2 and PM-3). The Gaussian function has the following three parameters: mean depth (h_m), dispersion (σ), and area (S). PM-2 operates on two fitting parameters: mean depth (h_m) and radius of quenching (R_c). PM-3 has an additional fitting parameter (f). C is a known value for quencher concentration.

One should keep in mind that the total depth-dependent fluorescence quenching profile measured in a standard experiment consists of two symmetrical components corresponding to *cis*- and *trans*-leaflet quenching (11, 12)

$$\ln \frac{F_0}{F(h)} = \text{QP}(h - h_m) + \text{QP}(h + h_m), \quad [4]$$

where QP stands for quenching profile from the right-hand side of Eqs. [1]–[3]. This equation utilizes the same number of parameters as the original equations, but allows accurate examination of deeply penetrating fluorophores. It turned out that, for the most systems analyzed in this study, the contribution of *trans*-leaflet quenching is negligible, and Eqs. [1]–[3] were used throughout most of the paper. Only the data for OmpA mutants were fitted to Eq. [1] in combination with Eq. [4]. Failure to account for *trans*-leaflet quenching was shown to dramatically affect the results in some simulated experiments (11, 15).

RESULTS AND DISCUSSION

Comparison of Different Methods of Data Analysis

Examples of the analysis of depth-dependent fluorescence quenching data are presented in Fig. 1. A membrane-anchoring nonpolar peptide of cytochrome b_5 mutant (NPP) was mixed with sonicated vesicles formed entirely with one of four different brominated lipids (4-5, 6-7, 9-10, or 11-12BPC) or POPC. Fluorescence of Trp-109 was measured and the logarithm of the ratio of intensities was plotted against the depth of

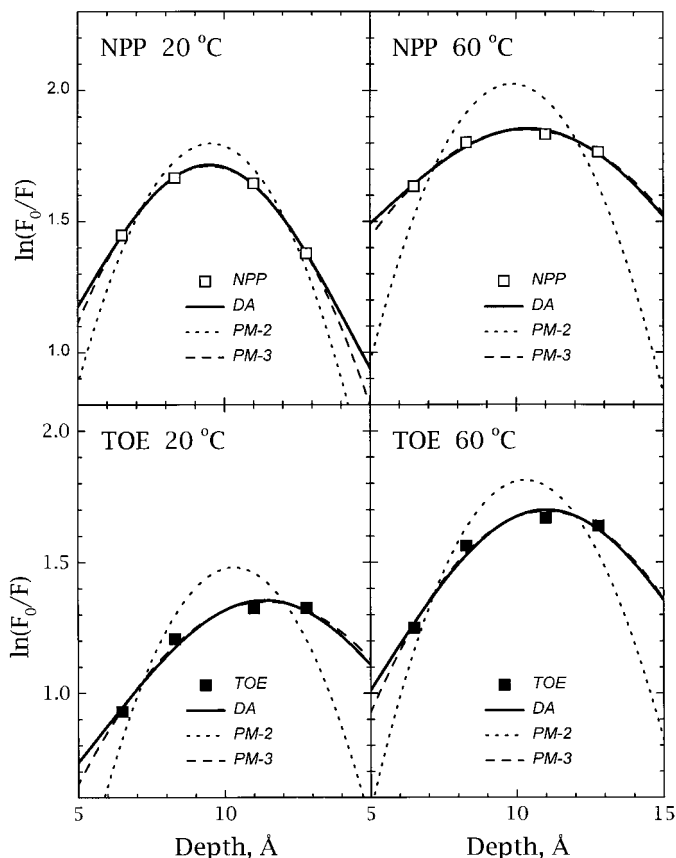


FIG. 1. Analysis of the depth-dependent quenching of TOE (lower panels) and cytochrome b_5 nonpolar peptide, NPP (upper panels), using different methods. Squares correspond to quenching of TOE or NPP fluorescence with the set of bromolipids measured at 20°C (left panels) and 60°C (right panels). Solid lines correspond to DA analysis; dotted lines correspond to PM-2; dashed lines correspond to PM-3. The summary of parameters is presented in Table 1. Both methods that operate with three fitting parameters (DA and PM-3) provide adequate description of the shape of the experimentally observed quenching profiles.

the quenchers known from independent diffraction measurements (16). The measurements were carried out at 20 and 60°C and results were compared to those of a model compound TOE measured at the same temperatures (14).

Four points on each plot in Fig. 1 constitute the experimentally observed quenching profile. In all cases raw data indicate the existence of a single extremum around 10–11 Å from the bilayer center. Despite this similarity, experimental quenching profiles differ in their sharpness and in the overall level of quenching, indicating existence of additional information besides the position of maximum. To extract this information the data were fitted using Eqs. [1]–[3] (lines in Fig. 1). It is immediately obvious that PM-2 is not capable of following the subtleties of experimental quenching profiles, while both methods that operate on three fitting parameters (DA and

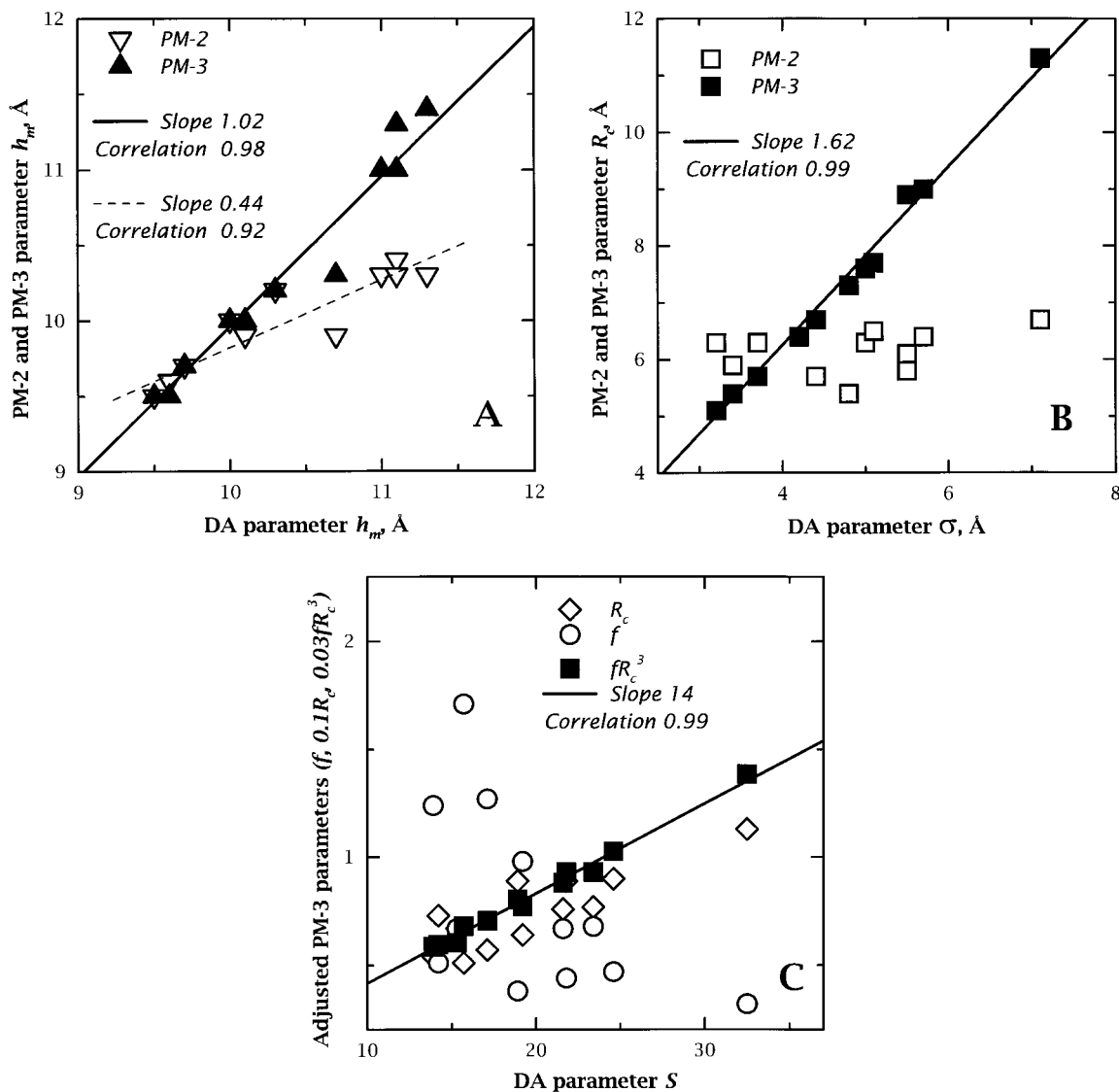


FIG. 2. Correlation between parameters of depth-dependent quenching obtained by different methods from the data presented in Table 1. PM-2 and PM-3 parameters representing position (A), width (B), and area (C) of the quenching profile are plotted against corresponding DA parameters. Correlation lines between PM-3 and DA parameters are shown as solid lines (see text for details.)

PM-3) give similarly good fits. Fitting parameters are summarized in Table 1. Despite the fact that the curves for DA and PM-3 almost coincide, there appears to be no direct correspondence between patterns of different parameters. For example, heating leads to increasing S for both NPP and TOE, but f can change either way: increase for TOE or decrease for NPP. This raises a question: How do the parameters obtained by different methods relate to each other and to properties of experimentally observed quenching profiles?

Correlation between DA and PM Parameters

To establish the correlation between the DA and PM parameters, Eqs. [1]–[3] were applied to the database

of 12 quenching profiles, both original and available in the literature (Table 1). All data were collected with the same set of quenchers specified above. In all cases DA and PM-3 gave equally good fits (not shown), similar to those in Fig. 1. PM-2 gave a good fit only in the single case of melittin at 45°C. To establish the correlation we plotted the PM parameters versus the DA parameters in Fig. 2.

The first and most obvious group of parameters is those related to the position of the quenching profile. The h_m values calculated by PM-3 (solid symbols) and PM-2 (open symbols) are plotted against the values calculated by DA in Fig. 2A. The correlation of PM-3 and DA data is extremely good. The slope of the correlation line (solid

line) practically equals one and the offset practically equals zero. The correlation of PM-2 data is somewhat worse (dashed line) and these data have a tendency to appear closer to the midpoint of the experimentally accessible region. Two correlation curves intercept at about 9.7 Å, which is exactly the averaged depth for this set of quenchers. This tendency is small—the maximal observed discrepancy is only 1 Å. However, it could be much larger if a two-point analysis is used instead of fitting of all experimental data (12).

The second group of parameters is related to the width of the quenching profile, and consists of σ parameter of the DA and R_c parameters of PM-2 and PM-3 (Fig. 2B). Here again PM-3 and DA give an excellent correlation, while R_c of PM-2 remains constant at about 6 Å. The correlation line for the DA-PM-3 pair (solid line) has a slope of 1.62 and the offset of zero within the error of determination, indicating a simple proportionality relation: $\sigma = 0.62 R_c$. Both parameters are related to the full width at the half height (FWHH) of the corresponding profile as follows: $\text{FWH-H}_{\text{DA}} \approx 2.35\sigma$; $\text{FWHH}_{\text{PM}} \approx 1.41 R_c$. Assuming that both methods are correctly describing the actual experimentally observed quenching profile, the parameters should be related as $\sigma \approx 0.60 R_c$. This predicted proportionality coefficient is very close to the observed one, suggesting that both methods consistently represent the width of the actual profile.

The third and less obvious group of parameters are related to the area of the quenching profile. Because PM-2 does not have a third parameter, only the correlation between parameters of DA and PM-3 was analyzed (Fig. 2C). Neither R_c nor f (open symbols) correlate with S , but fR_c^3 (closed symbols) does. Repeating the procedure described above for the width, one obtains for the area: $\text{Area}_{\text{DA}} = S$, $\text{Area}_{\text{PM}} \approx 4.19 C f R_c^3$. Thus, the predicted relation for the case of vesicles made entirely of bromolipids ($C = 1/70 \text{ Å}^2$) is $S \approx 0.060 f R_c^3$. The observed relation is $S \approx 0.070 f R_c^3$, suggesting that area predictions from two methods are close.

The analysis of the correlation plots, presented above, reveals that DA and PM-3 provide equivalent information on the experimentally observed quenching profiles and that the measures of these profiles, such as position, width, and area, can be obtained easily from either method. These measures can then be used to estimate the structural properties of the probe, e.g., tryptophan exposure.

Quantitation of the Lipid Exposure of Tryptophan Residue in NPP

According to Ref. (11) the area under the quenching profile, Area_{QP} , is a product of the inherent quenching constant, γ , determined by the nature of the quenching

mechanism; excited state lifetime in the absence of quenching, τ ; the degree to which the probe is exposed to a lipid phase, ω ; and the concentration of the quencher, C :

$$\text{Area}_{\text{QP}} = \gamma \cdot \omega \cdot \tau \cdot C. \quad [5]$$

We apply this formalism to estimate the exposure of Trp-109 in NPP. The variation of the exposure arises from the shielding of tryptophan side chains by the protein moiety. Therefore the relative exposure, Ω , could be estimated as the ratio of absolute exposures of tryptophan residue in a protein, ω_{NPP} , to that in TOE, ω_{TOE} (the concentrations of quenchers are the same in the two cases and the inherent quenching constant is assumed to be the same at each temperature, $\gamma_{\text{NPP}} = \gamma_{\text{TOE}}$):

$$\Omega = \frac{\omega_{\text{NPP}}}{\omega_{\text{TOE}}} = \frac{\text{Area}_{\text{QP}}^{\text{NPP}} \cdot \tau_{\text{TOE}}}{\text{Area}_{\text{QP}}^{\text{TOE}} \cdot \tau_{\text{NPP}}}. \quad [6]$$

If the lifetime measurements are not available, the ratio of τ 's can be approximated with the ratio of quantum yields, Q , of a protein and a model compound in a nonquenching lipid membrane:

$$\Omega = \frac{\omega_{\text{NPP}}}{\omega_{\text{TOE}}} = \frac{\text{Area}_{\text{QP}}^{\text{NPP}} \cdot Q_{\text{TOE}}}{\text{Area}_{\text{QP}}^{\text{TOE}} \cdot Q_{\text{NPP}}}. \quad [7]$$

The following values for the quantum yields for NPP and TOE when bound to POPC vesicles have been measured (expressed relative to the quantum yield of TOE at 20°C): $Q_{\text{TOE}}(60^\circ\text{C}) = 0.66$; $Q_{\text{NPP}}(20^\circ\text{C}) = 1.65$; $Q_{\text{TOE}}(60^\circ\text{C}) = 0.92$. These values were used together with the results for Area_{QP} from Table 1 to estimate the relative exposure of Trp-109 in NPP using Eq. [7]. Estimates based on DA parameters ($\text{Area}_{\text{DA}} = S$) are $\Omega(20^\circ\text{C}) = 0.69$, $\Omega(60^\circ\text{C}) = 0.95$. Estimates based on PM-3 parameters ($\text{Area}_{\text{PM}} \approx 4.19 C f R_c^3$) are similar: $\Omega(20^\circ\text{C}) = 0.66$, $\Omega(60^\circ\text{C}) = 0.97$.

As revealed by these calculations, NPP undergoes a temperature-controlled conformational change. At low temperature, Trp-109 is partially shielded from lipid by a peptide moiety. Upon heating, Trp-109 becomes completely exposed to the lipid. In addition, heating results in increasing width of the quenching profile (see Table 1), indicating a substantial heterogeneity in transverse position of a chromophore. This transition is fully reversible because the parameters of the quenching profile measured after cooling to 20°C are very close to those before heating (Table 1). This conformational change might be connected to temperature-induced conversion of the exchangeable ("loosely" bound) form of cytochrome b_5 to the nonexchangeable

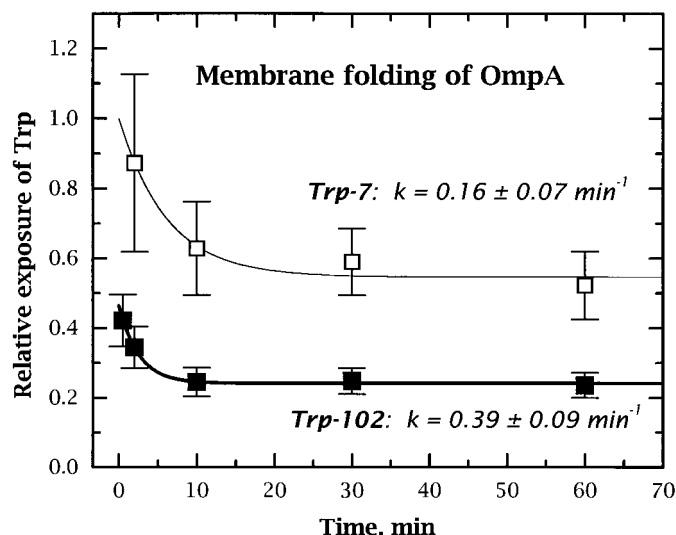


FIG. 3. Kinetic changes in relative exposure of tryptophan residues in two single tryptophan-containing mutants of OmpA. Kinetic quenching profiles reported by Kleinschmidt *et al.* (*Biochemistry* (1999) **38**, 5006–5016) collected at 40°C and kinetic changes in fluorescence without quenching were analyzed to extract the information on relative exposure of Trp-7 (open symbols) and Trp-102 (solid symbols) as described in the text. Solid lines correspond to error-weighted best fit single exponential approximations with kinetic constants specified in the figure. Data are normalized to the starting point of Trp-7 kinetic curve. Trp-102 appears to be noticeably shielded from the lipid environment as compared to Trp-7 throughout the folding event.

(“tightly” bound) form, forms which have dramatically different rates for exchange between membranes (5).

Kinetic Changes in Exposure of Trp-7 and Trp-102 upon Folding of OmpA

In addition to studies of the temperature-induced transitions, membrane quenching could be applied to kinetic studies of folding and insertion of membrane proteins and peptides. Previously we have applied DA to the kinetics of melittin insertion (17, 18). Recently Tamm and co-workers have applied this kinetic DA approach to follow the time course of the depth of penetration of tryptophans in the wild type of an outer membrane protein A (OmpA) and in several of its single tryptophan-containing mutants (6, 7). Their study contains all the necessary information to estimate changes in exposure of Trp-7 and Trp-102 to lipid during folding (Fig. 3) using the following procedure.

First, experimental quenching profiles (Figs. 4 and 5 of the Ref. (7)) were fitted to Eq. [1] in combination with Eq. [4] to obtain the *S* parameter at five different time points after the folding was initiated. The values for *S* parameter (and corresponding standard deviations obtained during the fit) were divided by the value of the fluorescence intensity measured in a nonquenching

lipid at corresponding points of time (Fig. 2 and Table 3 of (7)). Finally the difference in quantum yield of different mutants (Fig. 1 of (7)) was accounted for and the exposure values obtained were normalized to that for zero time extrapolation for W-7. This procedure is essentially the same as that used to evaluate exposure of Trp-109 in NPP with Eq. [7] (see above), with the only difference being that exposure is related not to TOE but to the highest value for the most exposed tryptophan.

The data for relative exposure for Trp7 and Trp-102 (Fig. 3, open and closed symbols, respectively) were fitted to a single exponential kinetic (solid lines) using the reciprocal of standard deviations as weighting function. It is essential to do correct error propagation, especially when analyzing kinetic data, because due to experimental limitations such data are inherently noisy. In both cases the obtained kinetic constants coincide with translocation constants reported by Kleinschmidt *et al.* (7) within confidence limits. This suggests that, at least for OmpA, kinetic changes of the average depth of the fluorophore and those for its exposure into lipid reflect the same folding process. Nevertheless, the analysis of the exposure provides additional insight on the folding event. Note that at all times Trp-102 appears to be significantly more shielded from the lipid (presumably by the protein moiety) compared to Trp-7 (see Fig. 3). Predominant interaction of Trp-7 with the lipid environment is consistent with its higher quantum yield in a non-brominated lipid, while Trp-102 shielded from the lipid is expected to be subjected to additional quenching from protein groups. Interestingly, according to the model of Tamm and co-workers (6, 7), Trp-102 is translocated across the bilayer, while Trp-7 remains on the *cis* side during folding. It would be interesting to see if translocation and additional protein shielding are correlated in other membrane proteins.

CONCLUSIONS

The essential points in determining the degree of lipid exposure of tryptophan residues in membrane proteins and peptides are summarized in the following protocol:

- Plot all of the experimentally available points of a quenching profile. If the profile is essentially flat or has a concave shape, then multiple conformations with different depths of penetration are present. This complicates a meaningful analysis of exposure (11). If the profile is convex (as in Fig. 1), then further mathematical analysis is possible.
- Use either DA (Eq. [1]) or PM-3 (Eq. [3]) in combination with Eq. [4] to fit the quenching profile of the protein and of the model compound (e.g., TOE) mea-

sured under the same conditions of temperature, pH, membrane composition, etc.

- Calculate the area under the quenching profile using $\text{Area}_{\text{DA}} = S$ or $\text{Area}_{\text{PM}} \approx 4.19 C f R_c^3$.

- Calculate the relative lipid exposure of tryptophan using additional lifetime (Eq. [6]) or quantum yield (Eq. [7]) measurements in the absence of quenching.

ACKNOWLEDGMENTS

I am very grateful to Drs. P. W. Holloway, E. London, and S. H. White for helpful discussions and to Mr. M. A. Myers for proof-reading the manuscript. My special thanks to Dr. W. C. Wimley for numerous discussions and valuable suggestions, and for comments on the manuscript. The research was supported by Grant GM-46823 (Professor S. H. White, PI) from the National Institutes of Health.

REFERENCES

1. Markello, T., Zlotnick, A., Everett, J., Tennyson, J., and Holloway, P. W. (1985) *Biochemistry* **24**, 2895–2901.
2. Berkhout, T. A., Rietveld, A., and de Kruijff, B. (1987) *Biochim. Biophys. Acta* **897**, 1–4.
3. Chung, L. A., Lear, J. D., and DeGrado, W. F. (1992) *Biochemistry* **31**, 6608–6616.
4. González-Mañas, J. M., Lakey, J. H., and Pattus, F. (1992) *Biochemistry* **31**, 7294–7300.
5. Ladokhin, A. S., Wang, L., Steggles, A. W., Malak, H., and Holloway, P. W. (1993) *Biochemistry* **32**, 6951–6956.
6. Kleinschmidt, J. H., and Tamm, L. K. (1999) *Biochemistry* **38**, 4996–5005.
7. Kleinschmidt, J. H., den Blaauwen, T., Driessen, A. J. M., and Tamm, L. K. (1999) *Biochemistry* **38**, 5006–5016.
8. Chattopadhyay, A., and London, E. (1987) *Biochemistry* **26**, 39–45.
9. Abrams, F. S., and London, E. (1992) *Biochemistry* **31**, 5312–5327.
10. Ladokhin, A. S. (1993) *Biophys. J.* **64**, A290.
11. Ladokhin, A. S. (1997) *Methods Enzymol.* **278**, 462–473.
12. Ladokhin, A. S. (1999) *Biophys. J.* **76**, 946–955.
13. Tretyachenko-Ladokhina, V. G., Ladokhin, A. S., Wang, L., Steggles, A. W., and Holloway, P. W. (1993) *Biochim. Biophys. Acta* **1153**, 163–169.
14. Ladokhin, A. S., and Holloway, P. W. (1995) *Biophys. J.* **69**, 506–517.
15. Kaiser, R. D., and London, E. (1998) *Biochemistry* **37**, 818–8190.
16. McIntosh, T. J., and Holloway, P. W. (1987) *Biochemistry* **26**, 1783–1788.
17. Ladokhin, A. S., and Holloway, P. W. (1995) *Ukrainian Biochem. J.* **67**, 34–40.
18. Ladokhin, A. S., Holloway, P. W., and Kostrzhevskaya, E. G. (1993) *J. Fluorescence* **3**, 195–197.